Mon. Not. R. Astron. Soc. **000**, 1–18 (2014) Printed 5 September 2014 (MN LATEX style file v2.2)

Evolution of Star Clusters on Eccentric Orbits

Maxwell Xu Cai[1,2⋆] Mark Gieles[3], Douglas C. Heggie[4] and Anna Lisa Varri[4⋆]

[1] *National Astronomical Observatories of China, Chinese Academy of Sciences, 20A Datun Rd., Chaoyang District, 100012, Beijing, P.R. Chin*

[2] *Kavli Institute for Astronomy and Astrophysics, Peking University, Yi He Yuan Lu 5, Haidian District, Beijing 100871, P.R. China*

[3] *Department of Physics, University of Surrey, Guildford GU2 7XH, UK*

[4] *School of Mathematics and Maxwell Institute for Mathematical Sciences, University of Edinburgh, Kings Buildings, Edinburgh, UK-EH9-3JZ*

5 September 2014

ABSTRACT

The evolution of star clusters are driven by both internal and external mechanisms. In this paper we investigate the role of galactic tidal fields as one of the external mechanisms that cause the dissolution of open clusters. The effect of galactic tidal fields is measured by the cluster life-time. While most previous studies modeled the trajectory of star clusters on circular orbits, we model the more general scenario where star clusters are moving along eccentric orbits, and thus experiencing time-dependent periodic tidal fields. We carry out a grid of simulations exploring the parameter space of different potentials, different orbital eccentricity and different size of star cluster. We scale the life-time of open clusters on eccentric orbits as a function of eccentricity, and obtained further results from the N-body scaling technique.

Key words: galaxies: star clusters: general; methods: numerical

1 INTRODUCTION

Star clusters are particularly interesting objects to study, as they provide valuable insights into stellar evolution, distance determination and many more. Pioneered by Chandrasekhar, various studies have been devoted to their dynamical evolution. The evolution of star clusters is driven by internal factors, such as two-body relaxation and stellar evolution, as well as external factors such as galactic tidal field. Recent studies showed that star clusters may

⋆ Also known as: Maxwell Tsai. E-mail: maxwell@nao.cas.cn

provide important clues for galaxy formation, in the senses that most stars, if not all, are formed in clusters. Star clusters, especially open clusters, have finite life times and as they dissolve, the released member stars become part of the galactic star population. Indeed, with the present of galactic tidal fields, the critical energy for stars to escape could be effectively lowered, allowing high energy stars to escape from the two Lagrangian points L1 and L2 (Tanikawa & Fukushige 2010).

Historically, studies of the dynamical evolution of star clusters heavily depended on analytical treatments. Indeed, this approach is elegant and useful to gain some physical intuition about these systems. However, due to the complexity of the galactic potential, almost all analytical studies are built upon certain assumptions. In recent years, thanks to the availability of computational technology and numerical algorithms, studying the dynamical evolution of star clusters with numerical simulations becomes more and more important. In this paper we investigate the evolution of star cluster under galactic tidal fields with `NBODY6tt`(Renaud, Gieles & Boily 2011), a variation of `NBODY6`(Aarseth 1999; Nitadori & Aarseth 2012) dedicated to study the tidal fields.

2 RELATED WORK

Baumgardt & Makino (2003) studied the dynamical evolution of star clusters in tidal fields with `NBODY4`.

According to the Baumgardt & Makino (2003) (hereafter, BM03), the dissolution time of star clusters moving in eccentric orbit as a function of eccentricity is (eq.8):

$$T_{diss}(e) = T_{diss}^{apo}(0)(1-e) \tag{1}$$

where $T_{diss}^{apo}(0)$ is the dissolution time of a star cluster moving on a circular orbit with radius similar to the apogalactic radii of the eccentric orbits. If the circular orbit is defined at the pericenter, the corresponding relation would be (BM03, eq9)

$$T_{diss}(e) = T_{diss}^{peri}(0)(1+e) \tag{2}$$

This shows that $T_{diss}^{peri}(0) < T_{diss}(e) < T_{diss}^{apo}(0)$, which implies that close passage is critical to the life time of star cluster.

On the other hand, equation (6) of BM03 implies that on the circular orbit with circular velocity v_c and radius R the cluster life-time is related to its orbital angular frequency $\Omega \equiv v_c/R$:

$$T_{diss} = k' \left[\frac{N}{\ln(\gamma N)}\right]^{x} \frac{R}{v_c} \propto \Omega^{-1} \tag{3}$$

According to Giersz & Heggie (1996), one could adopt $\gamma = 0.02$.

We would like to explore the following two questions:

(i) How does the evolution of a cluster on an eccentric orbit compare to one with the same lifetime, but on a circular orbit in the same potential?

(ii) How does the dissolution time of star clusters on eccentric orbits depend on Galactic potential?

To answer the above questions, we carry out a grid of simulations for open clusters with different number of stars (4096, 8192), different orbital eccentricity (0-0.8) and different galactic potentials (point mass Keplerian potential, singular isothermal potential and the potential yielded by a $\rho \sim R^{-1}$ density profile). This paper is organized as follows: section 3 presents the initial conditions for the star cluster setup, the galactic potential and the construction of the cluster orbits for given apocenter and eccentricity. The strategy for the simulation data analysis are described in section 4. The results and some preliminary interpretations are presented in section 5. We obtain some further results by scaling our raw simulation data, as shown in section 6. Finally our conclusions are summarized in section 7.

3 INITIAL CONDITIONS

3.1 Star cluster

In our simulations, the initial conditions have been sampled from a Plummer model. As a comparison, we simulated star clusters with 4096 particles and 8192 particles, respectively. In order to focus on the dynamical effects induced by the presence of an eternal tidal field, in our simulations we considered the evolution of equal mass particles and the effects of stellar evolution have been neglected.

3.2 Galaxy

We considered three types of galaxies, charactered by three different power indices of the enclosed mass profile:

$M(< R) = AR^{\lambda}$

Table 1. A summary of the general properties of the three types of galactic Potential used in the simulations.

λ	0 (point mass)	1 (Isothermal)	2 (Power-law Cusp)
Density profile	$\sim R^{-\infty}$	$\sim R^{-2}$	$\sim R^{-1}$
Enclosed mass	constant ($\sim R^0$)	$\sim R$	$\sim R^2$
Potential	$-GM/R$	$v_c^2 \ln(R)$	GM_0R/a^2
Tidal radius	$\sim R$	$\sim R^{2/3}$	$\sim R^{1/3}$
Orbital angular frequency	$\sim R^{-3/2}$	$\sim R^{-1}$	$\sim R^{-1/2}$

where $\lambda = 0, 1, 2$. The main properties of the three types of galaxies are summarized in Table 1.

3.3 Orbits

We constructed the orbits of star clusters with different eccentricity $e = 0.0, 0.2, 0.4.0.6, 0.8$ but same apocenter R_A. The apocenter is chosen such that at that radius the half mass radius r_h and the tidal radius r_t maintain a fixed ratio $f = r_h/r_t$, namely *filling factor*. In our simulations the filling factor is set to be the constant $f = 1/20$. The orbital details are tabularized in Appendix A.

3.3.1 Point mass galaxy ($\lambda = 0$)

The potential for the point mass galaxy is

$$\Phi(R) = -\frac{GM}{R}$$

The enclosed mass at any radius is always the total mass of the galaxy M_0:

$$M(< R) = M_0$$

The corresponding circular velocity is

$$\begin{aligned} v_c^2 &= \frac{GM(< R)}{R} \\ &= \frac{GM_0}{R} \end{aligned}$$

Since the total energy and total angular momentum must be conserved along the orbit, at the apocenter R_A and pericenter R_P

$$\frac{1}{2}v_A^2 - \frac{GM_0}{R_A} = \frac{1}{2}v_P^2 - \frac{GM_0}{R_P}$$

and from conservation of angular momentum we have

$$R_A v_A = R_P v_P$$

Finally we obtain

$$\begin{aligned} v_A^2(R_A, e) &= GM\left(\frac{2}{a} - \frac{1}{R}\right) \\ &= GM\frac{1-e}{R_A} \end{aligned}$$

which is the velocity at the apocenter as a function of apocenter distance to the galactic center R_A and orbital eccentricity $e(0 <= e <= 1)$.

3.3.2 Singular Isothermal Galaxy ($\lambda = 1$)

The potential for the singular isothermal galaxy is

$$\Phi(R) = v_c^2 \ln R$$

According to the Poisson equation,

$$\begin{aligned} \rho(R) &= \frac{\nabla^2 \Phi}{4\pi G} \\ &= \frac{\frac{1}{R^2}\frac{\partial}{\partial R}R^2\frac{\partial}{\partial R}v_c^2 \ln R}{4\pi G} \\ &= \frac{v_c^2}{4\pi G R^2} \end{aligned}$$

The enclosed mass therefore should be

$$M(R) = \int_0^R 4\pi R^2 \rho(R) dR = \int_0^R 4\pi R^2 \frac{v_c^2}{4\pi G R^2} dR = \frac{v_c^2}{G} R$$

The circular velocity of such a galaxy is constant, as one can easily see. Given that the total energy and total angular momentum must be conserved along the orbit, at the apocenter R_A and pericenter R_P

$$\frac{1}{2}v_A^2 + v_c^2 \ln(R) = \frac{1}{2}v_P^2 + v_c^2 \ln(R)$$

and

$$R_A v_A = R_P v_P$$

Finally we obtain

$$\begin{aligned} v_A^2(R_A, e) &= \frac{2v_c^2 \ln(r_a/r_p)}{(r_a/r_p)^2 - 1} \\ &= \frac{2v_c^2 \ln\left(\frac{1+e}{1-e}\right)}{\left(\frac{1+e}{1-e}\right)^2 - 1} \end{aligned}$$

which is the velocity at the apocenter as a function of apocenter distance to the galactic center R_A and orbital eccentricity $e(e > 0)$.

3.3.3 Power-law Cusp Galaxy ($\lambda = 2$)

Observations of luminosity profiles of ellipticals and bulges are often well described by the empirical formula $I \propto \exp(-const \times R^{1/4})$ (de Vaucouleurs 1948). However further observations of the recent decades indicated that the majority of galaxies may have a constant slope almost all the way into the center (e.g. Lauer et al. (1992); Crane & Stiavelli 1993). To match the observation, two models introduced by Jaffe (1983) and Hernquist (1990) argue that the surface density in the central region is proportional to R^{-1} and $\ln R^{-1}$. Those models are generalized by Dehnen (1993). Inspired by these models, we are interested to investigate open cluster around the central region with eccentric orbits.

Assume that the density profile takes the following form

$$\rho = \frac{M_0}{2\pi a^2} R^{-1}$$

for $R < a$, otherwise $\rho = 0$. The enclosed mass within radius R is

$$\begin{aligned} M(R) &= \int_0^r 4\pi R^2 \rho(R) dR \\ &= \int_0^R 4\pi R^2 \frac{M_0}{2\pi a^2} R^{-1} dR \\ &= M_0 \frac{R^2}{a^2} \end{aligned}$$

For spherical systems, the potential at radius R takes the form

$$\Phi(R) = -4\pi G \left[\frac{1}{R} \int_0^R \rho(R') R'^2 dR' + \int_R^a \rho(R') R' dR' \right]$$

The first term on the RHS is the potential yielded by the enclosed mass within the sphere of radius R; the second term on the RHS is the potential generated by a shell of material from R to some radius a. To be specific, for $R \leq a$,

$$\begin{aligned} \Phi(R) &= -2G \frac{M}{a^2} \left[\frac{1}{R} \int_0^R dR' R' + \int_R^a dR' \right] \\ &= \frac{GM}{a} \left[\frac{R}{a} - 2 \right] \\ &\propto \frac{GMR}{a^2} \end{aligned}$$

For $R > a$, according to Newton's second theorem we have

$$\Phi(R) = -\frac{GM_0}{R}$$

The orbit is assumed to lie within the region $R < a$, and that we ignore the constant term in the potential. The corresponding circular velocity for this simplified potential is

$$v_c^2(R) = \frac{GM(<R)}{R} = \frac{GM_0}{a^2}R$$

Since there is no dissipation, the conservations of total energy and total angular momentum must again hold alone the entire orbit, hence at the apocenter R_A and pericenter R_P:

$$\frac{1}{2}v_A^2 + \frac{GM_0}{R_A} = \frac{1}{2}v_P^2 + \frac{GM_0}{R_P}$$

and

$$R_A v_A = R_P v_P$$

Finally we obtain

$$v_A^2 = \frac{2\frac{GM_0}{a^2}\left[R_A - R_A\left(\frac{1-e}{1+e}\right)\right]}{1-\left(\frac{1+e}{1-e}\right)^2}$$

which is the velocity at the apocenter as a function of apocenter distance to the galactic center R_A and orbital eccentricity $e(e > 0)$.

4 DATA PROCESSING AND ANALYSIS

We consider a star cluster as dissolved when only less than 10% of the initial mass is bound. In our simulations a particle is considered as bound as long as its total energy is negative and it is confined within the tidal radius. As such, two characteristic life-time for star clusters are defined as:

- Life-time (dissolution time): time during which a star cluster lose 90% of its initial mass;
- Half life-time: time during which a star cluster lose 50% of its initial mass.

The mass-loss rate of star cluster under galactic tidal fields is usually non-linear. In fact, by plotting the bound mass M_{bound} against the evolution time T, one could fit the curve with a gaussian function (see Figure 1). It is therefore useful to characterize the dissolution process of star clusters with two characteristic timescales, instead of using only the dissolution time.

On eccentric orbits, the tidal radius of a star cluster is a function of time (Bertin & Varri 2008; Tanikawa & Fukushige 2010; Webb et al. 2014):

$$R_t^3 = \frac{GM_c(<R(t))}{(3-\lambda)\Omega^2}$$

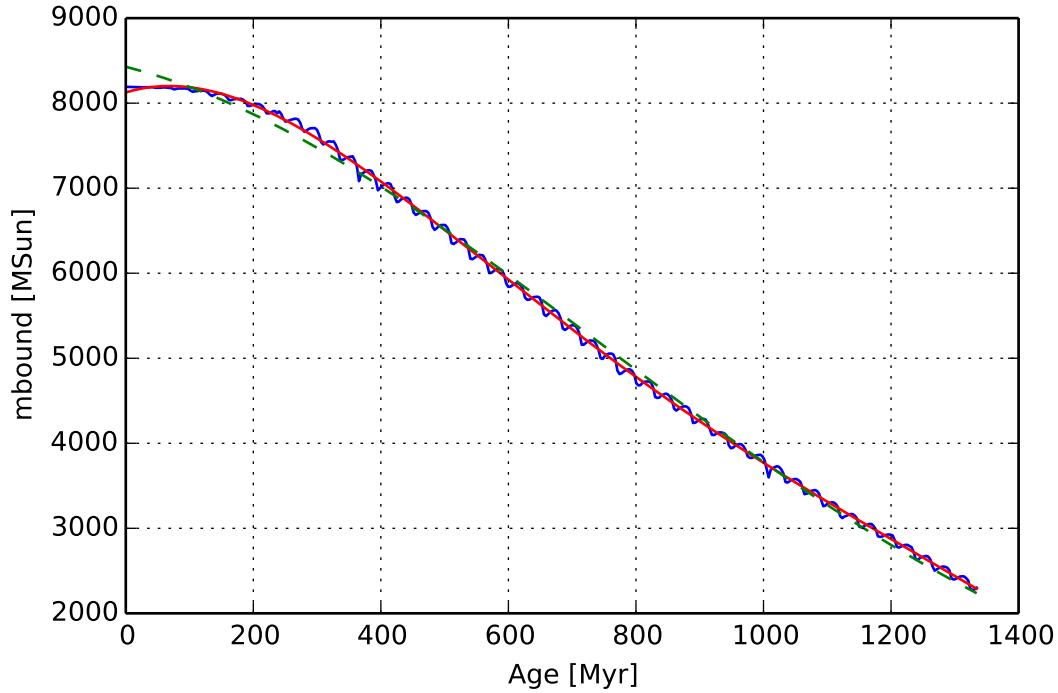

Figure 1. Bound mass of a star cluster on an eccentric orbit ($e = 0.8$). The potential is $\lambda = 2$. The oscillation of bound mass is due to the pericenter passages, at which the cluster is close to the galactic center and therefore experiences strong tidal stripping.

where λ is the power index of the enclosed mass within radius R, as defined in Section 2, and M_c is the total mass of the cluster. The tidal radius therefore changes rapidly during the pericenter passage, making it potentially tricky to define bound stars. The energy of the individual stars is defined as $e = 0.5v^2 + \phi_c(r)$, where v is the velocity of the stars in the centre of mass frame of the cluster and $\phi_c(r)$ is the specific potential of the star at radius r from the cluster centre. Here we only consider the contribution to ϕ_c of the other cluster stars, i.e. the contribution due to the galaxy is ignored (Renaud, Gieles & Boily 2011).

5 RESULTS AND INTERPRETATIONS

The plots of the half life-time and dissolution time as a function of cluster orbit eccentricity are presented in Figure 2 and Figure 3, respectively. Both figures suggest that

(i) the strength of galactic potential decrease as the λ index increases, as one could see that star clusters in the the point mass galaxy ($\lambda = 0$) has shortest life time, while in the the power-law cusp galaxy star clusters have the longest life-time.

(ii) More massive star cluster will have longer life-time than the less massive ones.

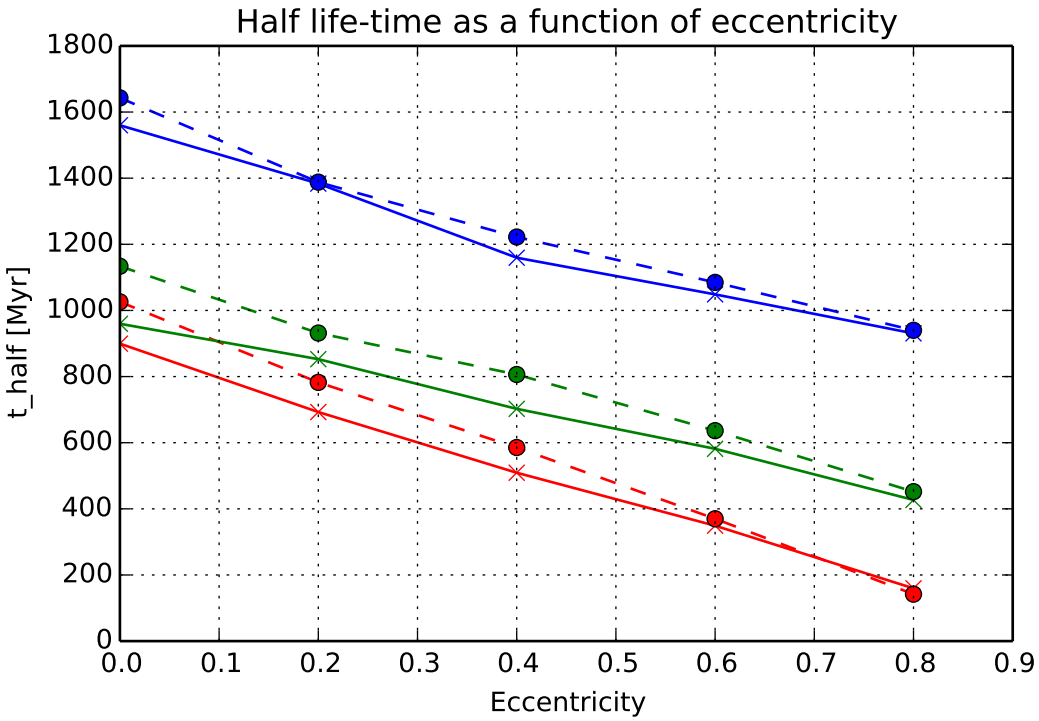

Figure 2. Half life-time as a function of eccentricity. Color: red($\lambda = 0$); green($\lambda = 1$); blue($\lambda = 2$). Line style: solid lines (4k simulations); Dash line (8k simulations).

The two direct conclusions drawn from the raw data plots are quite intuitive. For the same tidal radius, the shape of the Roche volume is different for the 3 galaxies. For the PM galaxy the "opening" in phase space is larger, and for $\lambda = 2$ it is smallest, so it is gets harder to escape for larger λ. Consequently, star cluster are less affected by the galactic tidal field and have longer dissolution time.

The life-time can also be expressed with dimensionless units. Figure 4 and Figure 5 show the normalized life time, where the life-time of star cluster on eccentric orbits are normalized to the corresponding life time of circular orbits. Again, each curve represents a series of simulations with the same galactic potential, same number of stars, same apocenter distance but different eccentricities.

Note that the normalization results largely depend on the quality of the initial data point. In our case the life-time of the circular orbits should be precise enough to ensure that the eccentric life-time are normalized properly. In our simulations star clusters moving on circular orbits have reasonable energy conservation. The bound mass is relatively straightforward to determine because the tidal radius is constant. Therefore the normalized results should be reliable in general.

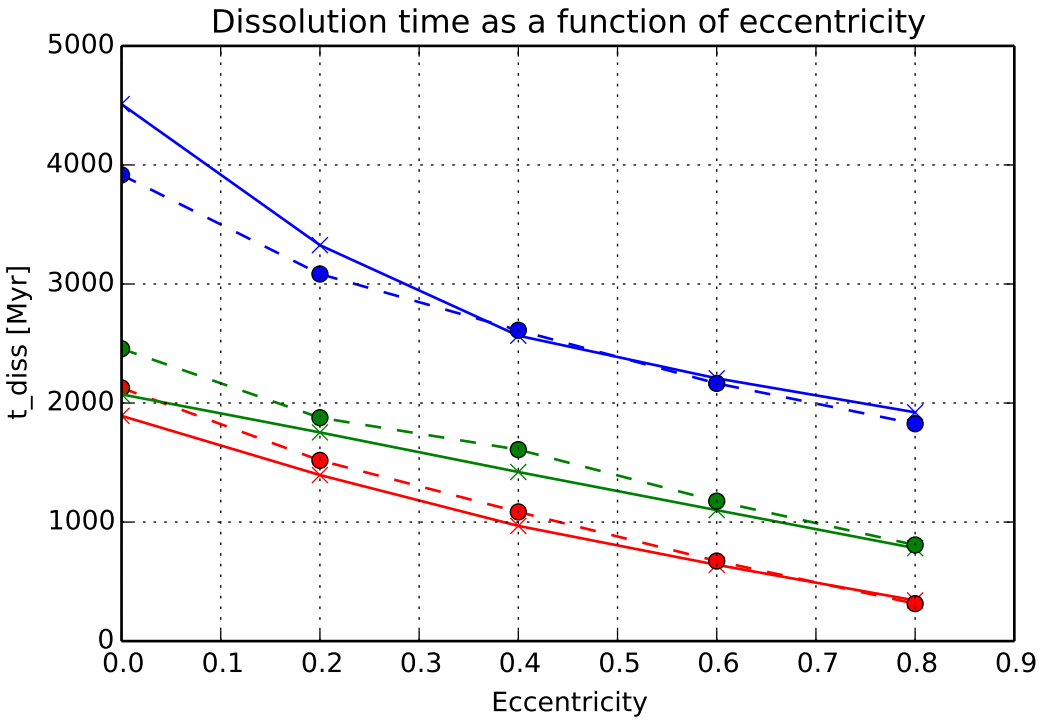

Figure 3. Dissolution time as a function of eccentricity. Legend: same as Figure 2.

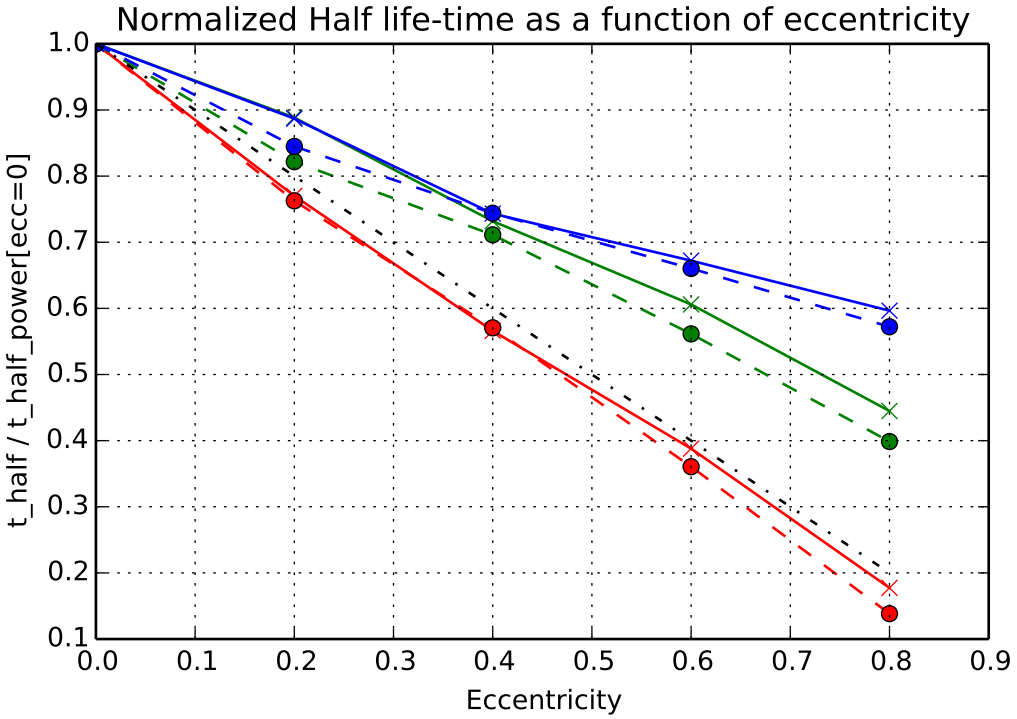

Figure 4. Half life-time normalized to the life-time of the circular orbits. Legend: same as Figure 2.

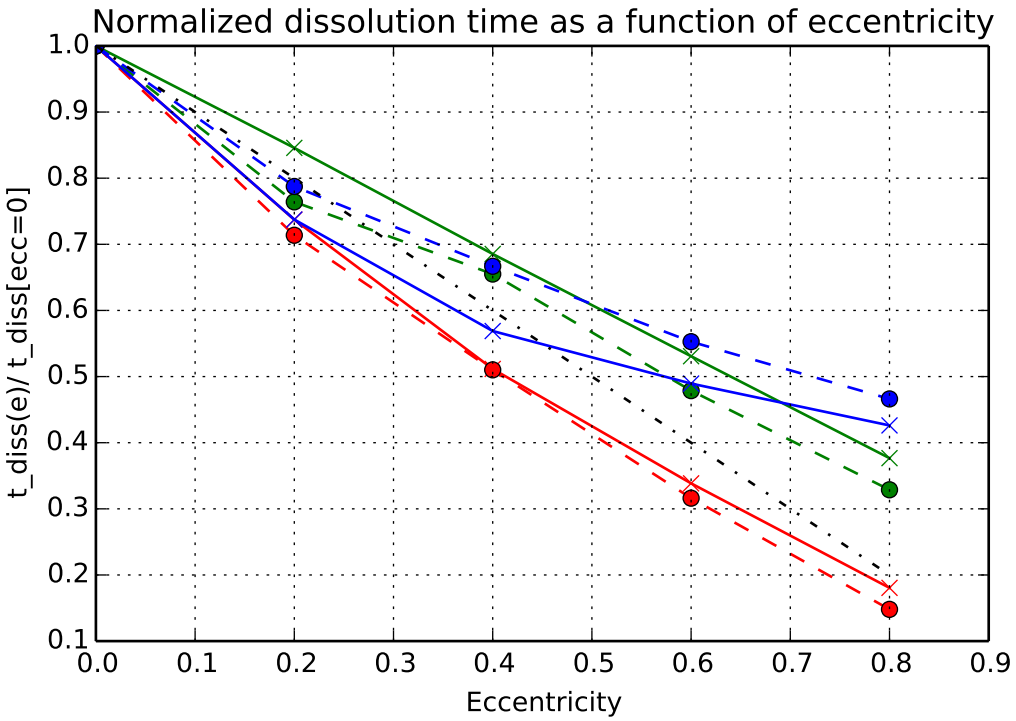

Figure 5. Dissolution time normalized to the life-time of the circular orbits. Legend: same as Figure 2.

The normalized results show some deviations from BM03. BM03 states that the life-time of star clusters in the isothermal galaxy (i.e. $\lambda = 1$) scales as $T_{diss}(e) = T_{diss}(0)(1 - e)$, as denoted by the black dash-dot line in Figure 5. However, it is important to notice that the initial conditions used in BM03 simulations differ from our simulations by the following aspects:

- N: BM03 carried out simulations with 32k and 64k stars; due to the time limitation of the ISIMA project we only managed to carry out simulation of 4k and 8k stars.
- Filling factors: BM03 sets star clusters of different mass at the same apogalactic distance, resulting to different filling factors; we instead keep the filling factor constant, resulting to different apogalactic distances for star clusters with different total mass.
- IMF: BM03 uses the Kroupa (2001) IMF. In our simulation we use the equal-mass model.
- Stellar evolution: BM03 takes stellar evolution into account. Our simulations are pure N-body.
- Density profile: BM03 uses the King profile with $W_0 = 5.0$ and $W_0 = 7.0$. We use the Plummer model.

6 FURTHER RESULTS FROM N-BODY SCALING

6.1 N-body Scaling Revisited

Many star cluster codes adopt the so-called N-body units, or Henon units (Henon 1971), as their internal unit systems. The adaptation of this common unit system makes comparison of simulation results from different authors rather straightforward. The Henon unit system assumes that the system is in virial equilibrium, and define the following fundamental physical constants:

$$\begin{aligned} G &= 1 \\ M &= 1 \\ E &= -0.25 \end{aligned}$$

respectively, where G is the gravitational constant, M is the total mass, and E is the total energy of the system. The corresponding units of mass, length and time are then

$$\begin{aligned} U_m &= M \\ U_l &= -\frac{GM^2}{4E} \\ U_t &= \frac{GM^{5/2}}{(-4E)^{3/2}} \end{aligned}$$

according to Heggie & Mathieu (1986). A cluster is essentially defined by the two global parameters R_V and M_S together with N, where M_S is the mean stellar mass in solar units. Therefore the fundamental relation between Henon units and physical units are

$$\begin{aligned} \tilde{r} &= R_V r \\ \tilde{m} &= N M_S m \end{aligned}$$

according to Aarseth (2003). This relation is actually a scaling relation, because by defining the scaling factors R_V and M_S one could scale the N-body model in arbitrary ways.

6.2 Result I: Life-time of Star Clusters with the Same Semi-major Axis

Recall that in our simulations we constructed cluster orbits with the same apocenter but different eccentricity. These family of orbits therefore will have different semi-major axes. It is desirable to see how the eccentricity affects the life-time of star clusters if star clusters are placed in orbits with the same semi-major axis but different eccentricities. Taking the

advantage of the N-body scaling, it is not necessary to rerun any simulations; rather, the corresponding life-time can be derived directly from the existing data.

The scaling follows as below: for orbits of given apocenter distance R_A, the semi-major axis a is a function eccentricity e:

$$\begin{aligned} a_{R_A,e} &= \mathcal{F}_{R_A}(e) \\ &= \left(\frac{1-e}{1+e}R_A + R_A\right)/2 \end{aligned}$$

To scale $a_{R_A,e}$ to a given semi-major axis $\tilde{a}$, or in another word, to set $\tilde{a} = R_* a_{R_A,e}$, the length scaling factor is

$$R_* = \tilde{a}/a_{R_A,e}$$

Since the orbital period for a circular orbit is given by

$$T = 2\pi/\Omega = \frac{2\pi R^{3/2}}{\sqrt{GM\,(<R)}}$$

the corresponding scaling of time can be derived by plugging in the enclosed mass profile $M(<R)$ in the three types of galaxy, respectively. Table 1 lists the orbital frequencies for three types of galaxies. Since Ω is proportional to $R^{-3/2}, R^{-1}, R^{-1/2}$ for $\lambda = 0, 1, 2$ respectively, it is easy to see that the orbital period is proportional to $R^{3/2}, R, R^{1/2}$ for $\lambda = 0, 1, 2$, respectively. At this point, the scaling relationship of length and time units for the three different types of galaxies can be tabularized as below:

	Length Scaling	Time Scaling
$\lambda = 0$	$\tilde{a} = \alpha a_{R_A,e}$	$\tilde{T} = \alpha^{3/2} T_{R_A,e}$
$\lambda = 1$	$\tilde{a} = \alpha a_{R_A,e}$	$\tilde{T} = \alpha T_{R_A,e}$
$\lambda = 2$	$\tilde{a} = \alpha a_{R_A,e}$	$\tilde{T} = \alpha^{1/2} T_{R_A,e}$

Figure 6 and Figure 7 shows the scaled half life-time and life-time of star cluster moving on orbits with the same semi-major axis but different eccentricity, respectively.

Likewise, we again normalize those life-time to the circular life-time, shown in Figure 8 and 9, respectively.

The scaled data suggests that the eccentricity dependence decreases as the λ index increases, which is the same as the same apocenter case. One could also see that higher eccentricity results to shorter life time. More interestingly, from the normalized plots one

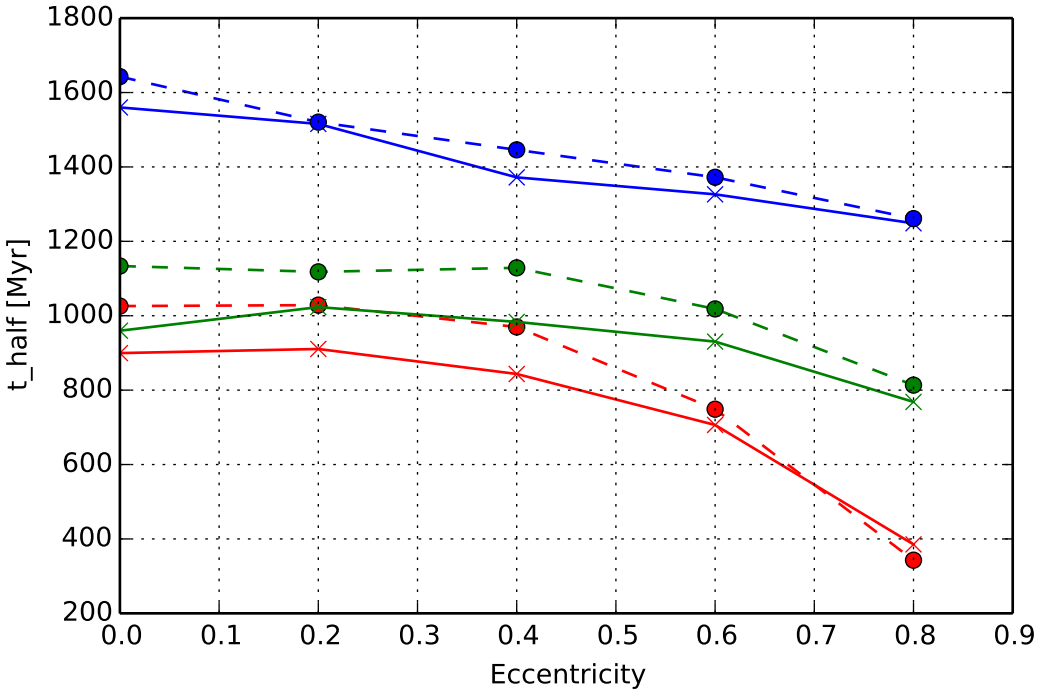

Figure 6. Half life-time scaled to the same semi-major axis. Legend: same as Figure 2.

could see that different eccentricity will affect the cluster life-time on different magnitude, depending on the type of galactic potential.

7 CONCLUSIONS

Star clusters dissolve as a result of both internal mechanisms and external mechanisms. While the internal mechanisms are being studied for decades, detailed investigations of external mechanisms such as external tidal fields have been generally difficult until the last two decades, thanks to the availability of high performance computing technologies. In this project we mainly focused on the life-time of star clusters on eccentric orbits. We explored the parameter space by running a grid of simulations with different total number of particles, different galactic potentials and different orbital eccentricities. Our simulations show that the life time of star clusters depends on the eccentricity of its orbit, the galactic potential as well as the number of stars in the cluster. According to the previous investigations, there are further complications that could affect the life-time, such as the initial concentration, and the Roche filling factor. Due to the limitation of time during the ISIMA2014 program, we had to limit our simulations to pure N-body equal mass small open clusters. Nevertheless, it is still possible to obtain some results from those simulations, which are generally consistent

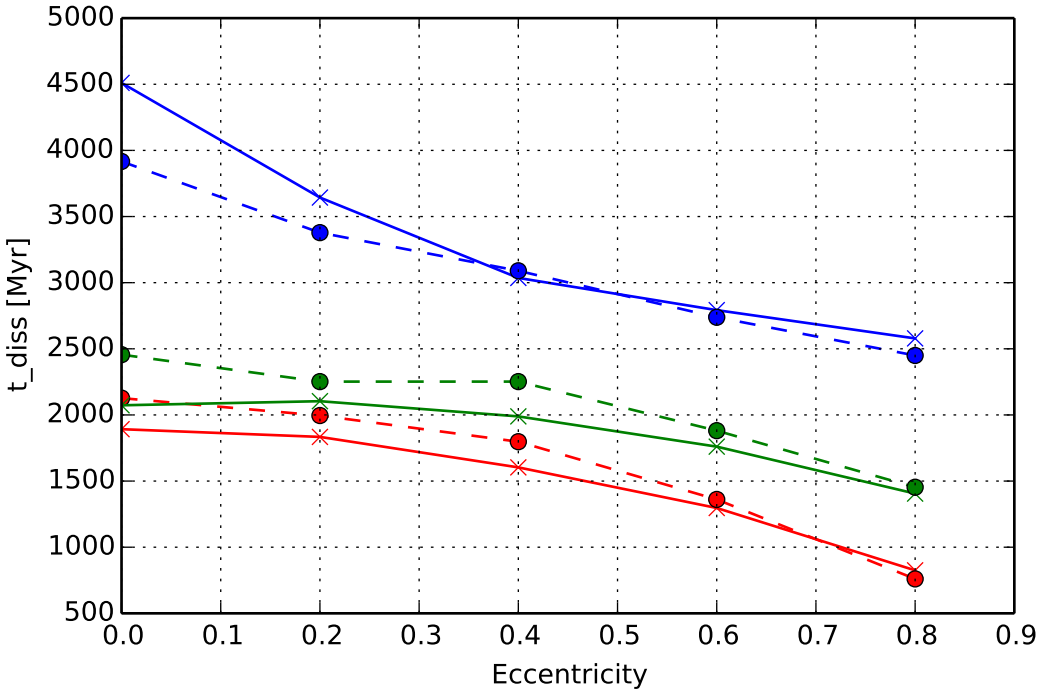

Figure 7. Dissolution time scaled to the same semi-major axis. Legend: same as Figure 2.

with the literatures. we took the advantage of the N-body scaling technical and obtain further results from that.

As shown from the simulations, multiple factors may contribute to the life-time of clusters. We would therefore argue that the results of BM03 might not be robust enough for generic cases.

8 ACKNOWLEDGEMENTS

This work was initiated during the International Summer-Institute for Modeling in Astrophysics (ISIMA) in 2014, hosted at CITA at the University of Toronto. We gratefully thank the organizers of ISIMA, especially Prof. Pascale Garaud for the kind support of our participation. We thank CITA for hosting the ISIMA program. We thank Florent Renaud, Rainer Spurzem and Thijs Kouwenhoven for useful discussions. MXC acknowledges supported by Chinese Academy of Sciences Grant Number 2009S1-5, and through the "Thousand Talents" (Qianren) program of China (R. Spurzem).

REFERENCES

Aarseth, S. J., 1999, PASP, 111, 1333

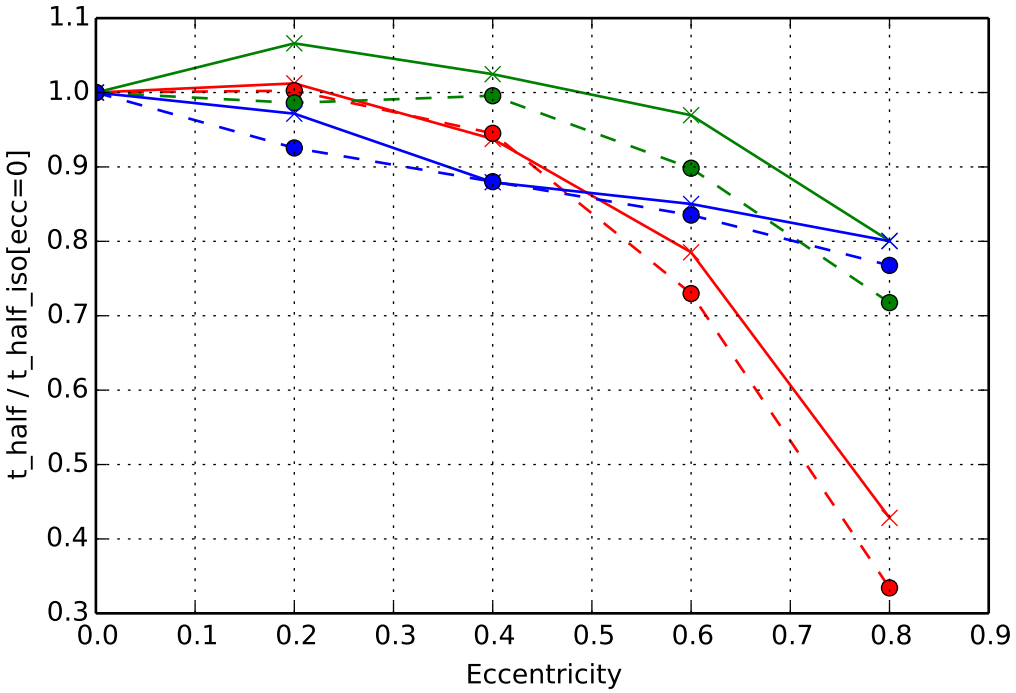

Figure 8. Scaled half life-time normalized to the same semi-major axis. Legend: same as Figure 2.

Baumgardt, H., Makino, J., 2003, MNRAS, 340, 227

Baumgardt, H., 2001, MNRAS, 325, 1323

Bertin, G., Varri, A. L., 2008, ApJ, 689, 1005

Dehnen, 1993, MNRAS, 265, 250

Baumgardt, H., Makino, J., 2003, MNRAS, 340, 227

Giersz, M., Heggie, D. C., 1996, MNRAS, 279, 1037

Heggie, D. C., Mathieu, R, D., 1996, MNRAS, 279, 1037

Henon, M.H., 1971, AP&SS, 14, 151

Hernquist, L., 1990, MNRAS, 356, 359

Jaffe, W., 1983, MNRAS, 202, 995

Lauer, T.R. et al., 1992, AJ, 104, 552

Aarseth, S. J., 1999, PASP, 111, 1333

Renaud, F., Gieles, M., Boily, C.M̃., 2011, MNRAS, 418, 759

Tanikawa, A., Fukushige, T., 2010, PASJ, 62, 1215

Webb, J. et al., 2014, MNRAS, 442, 1569

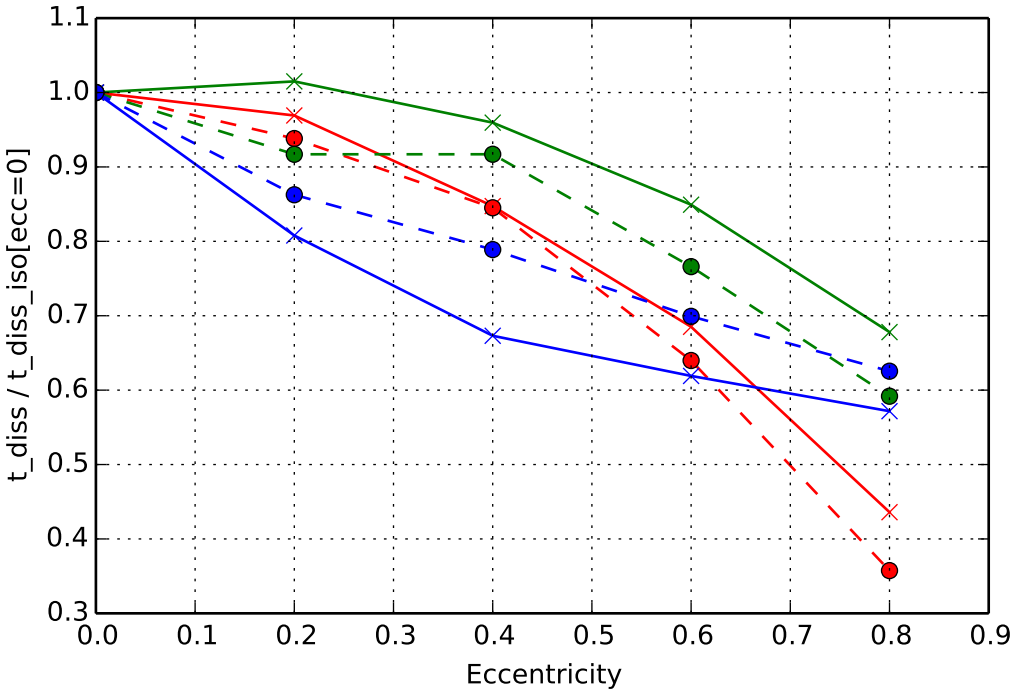

Figure 9. Scaled dissolution time normalized to the dissolution time of the circular orbits. Legend: same as Figure 2.

Table A1. Initial conditions of the cluster orbits. Each table cell contains two values. The value on the first line is the distance from the apocenter to the galactic center in kpc; the second line is the velocity at the apocenter in km/s. The mass of each star is 1 solar mass. The initial virial radius of all models is 1pc; the initial half-mass radius of all models is 0.78pc.

λ	$\lambda = 0$		$\lambda = 1$		$\lambda = 2$	
N	4096	8192	4096	8192	4096	8192
$e = 0.0$	3.029 119	2.404 134	4.567 220	3.229 220	4 272	2 193
$e = 0.2$	3.029 107	2.404 120	4.567 177	3.229 177	4 199	2 141
$e = 0.4$	3.029 92	2.404 104	4.567 136	3.229 136	4 138	2 98
$e = 0.6$	3.029 75	2.404 85	4.567 95	3.229 95	4 86	2 61
$e = 0.8$	3.029 53	2.404 60	4.567 52	3.229 52	4 41	2 29

APPENDIX A: VELOCITY AND APOCENTER OF THE STAR CLUSTER ORBITS

This paper has been typeset from a TEX/ LATEX file prepared by the author.